

# **Integrating the *IMSA* with Bayesian Compressive Sensing for Solving Inverse Scattering Problems**

N. Anselmi, L. Poli, G. Oliveri, and A. Massa

## **Abstract**

A novel microwave imaging technique is proposed in this work for solving 2D transverse magnetic inverse scattering problems under the first order Born approximation. The developed strategy exploits the well-known regularization capabilities of Bayesian compressive sensing (*BCS*) and the progressively acquired information through a multi-resolution iterative approach. Towards this end, a customized relevance vector machine (*RVM*) solver is implemented to iteratively improve the *BCS* solution accuracy within the identified region of interest (*RoI*). Selected numerical results are shown to verify the effectiveness of the proposed methodology.

# 1 Numerical Results

## 1.1 Inhomogeneous Square Object, $\ell = 1.5\lambda$

### Test Case Description

#### Direct solver:

- Side of the investigation domain:  $L = 6.0\lambda$
- Cubic domain divided in  $\sqrt{D} \times \sqrt{D}$  cells
- Number of cells for the direct solver:  $D = 1600$  (discretization =  $\lambda/10$ )

#### Investigation domain:

- Cubic domain divided in  $\sqrt{N} \times \sqrt{N}$  cells
- Number of cells for the inversion:
  - First Step IMSA:  $N^{(1)} = 100$  (discretization =  $\lambda/10$ )
  - Following Steps IMSA:  $N^{(i)}$  not fixed, defined according to the estimated *RoI*  $\mathcal{D}^{(i)}$

#### Measurement domain:

- Total number of measurements:  $M = 60$
- Measurement points placed on circles of radius  $\rho = 4.5\lambda$

#### Sources:

- Plane waves
- Number of views:  $V = 60$ ;  $\theta_{inc}^v = 0^\circ + (v - 1) \times (360/V)$
- Amplitude:  $A = 1.0$
- Frequency:  $F = 300$  MHz ( $\lambda = 1$ )

#### Background:

- $\epsilon_r = 1.0$
- $\sigma = 0$  [S/m]

#### Scatterer

- Inhomogeneous square object,  $\ell = 1.5\lambda$
- $\epsilon_r^{(1)} \in \{1.02, 1.04, 1.06, 1.08, 1.10, 1.12, 1.14, 1.16, 1.20\}$  (internal circle)  
 $\epsilon_r^{(2)} = \frac{\epsilon_r^{(1)}}{2}$  (central circle)  
 $\epsilon_r^{(3)} = \frac{\epsilon_r^{(1)}}{4}$  (external circle)
- $\sigma = 0$  [S/m]

### 1.1.1 Inhomogeneous Square Object, $\ell = 1.5\lambda$ , $\tau^{(1)} = 0.02$ - IMSA-BCS reconstructed profiles

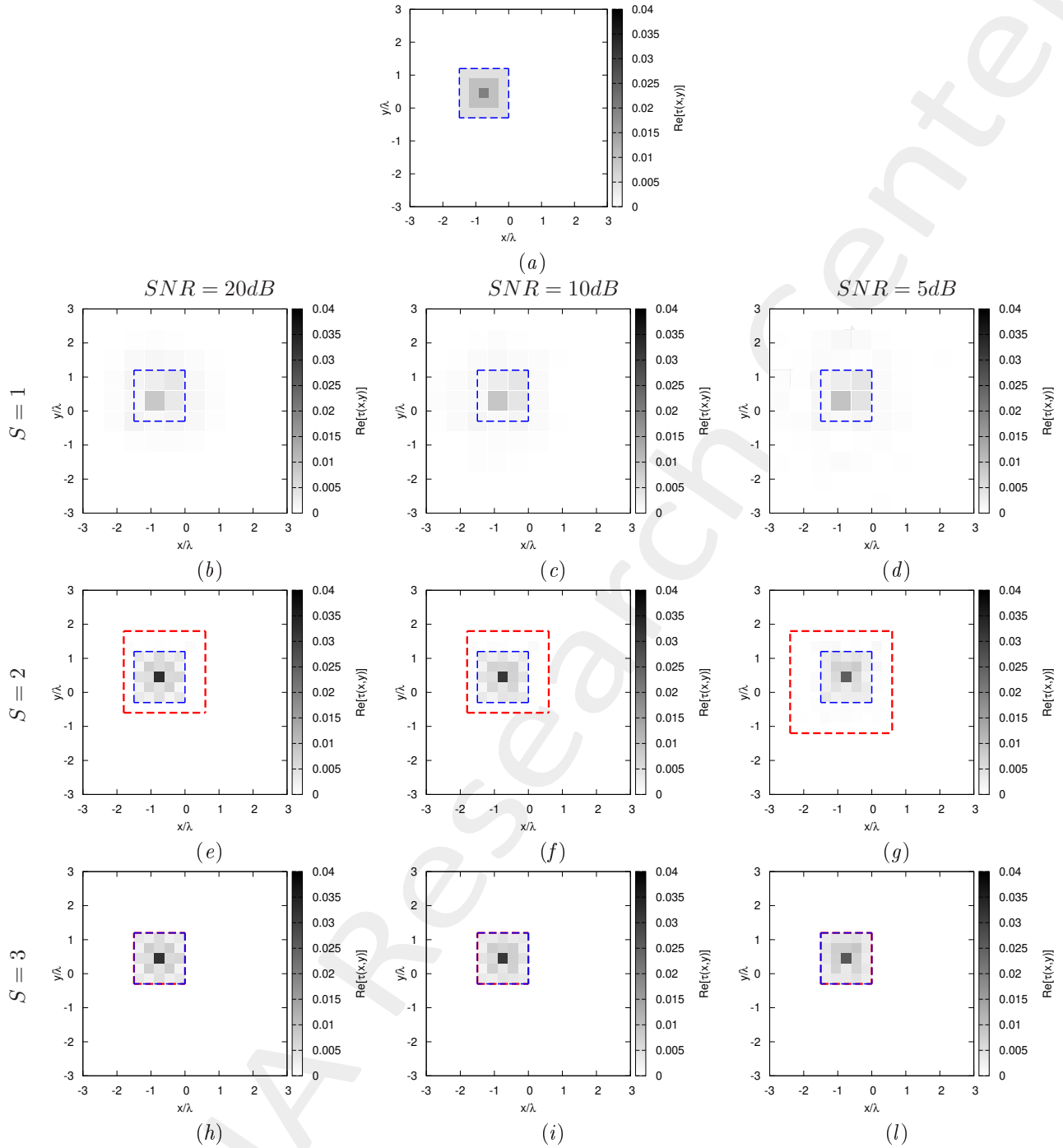


Figure 1: *Inhomogeneous Square Object*,  $\ell = 1.5\lambda$ ,  $\tau = 0.02$  - (a) Actual profile and (b)-(o) IMSA-BCS reconstructed profiles for (b)(e)(h)  $SNR = 20$  [dB], (c)(f)(i)  $SNR = 10$  [dB] and (d)(g)(l)  $SNR = 5$  [dB] at the step (b)-(d)  $S = 1$ , (e)-(g)  $S = 2$ , and (h)-(l)  $S = 3$ .

	$SNR = 50dB$			
	$S = 1$	$S = 2$	$S = 3$	$S = 4$
$\xi_{tot}$	$4.01 \times 10^{-4}$	$1.93 \times 10^{-4}$	$1.74 \times 10^{-4}$	$1.74 \times 10^{-4}$
$\xi_{int}$	$3.57 \times 10^{-3}$	$2.95 \times 10^{-3}$	$2.78 \times 10^{-3}$	$2.78 \times 10^{-3}$
$\xi_{ext}$	$1.89 \times 10^{-4}$	$9.03 \times 10^{-6}$	$0.00 \times 10^{-1}$	$0.00 \times 10^{-1}$
	$SNR = 20dB$			
	$S = 1$	$S = 2$	$S = 3$	$S = 4$
$\xi_{tot}$	$4.11 \times 10^{-4}$	$1.99 \times 10^{-4}$	$1.72 \times 10^{-4}$	$1.72 \times 10^{-4}$
$\xi_{int}$	$3.64 \times 10^{-3}$	$3.00 \times 10^{-3}$	$2.75 \times 10^{-3}$	$2.75 \times 10^{-3}$
$\xi_{ext}$	$1.95 \times 10^{-4}$	$1.17 \times 10^{-5}$	$0.00 \times 10^{-1}$	$0.00 \times 10^{-1}$
	$SNR = 10dB$			
	$S = 1$	$S = 2$	$S = 3$	$S = 4$
$\xi_{tot}$	$3.98 \times 10^{-4}$	$1.98 \times 10^{-4}$	$1.58 \times 10^{-4}$	$1.58 \times 10^{-4}$
$\xi_{int}$	$3.46 \times 10^{-3}$	$2.87 \times 10^{-3}$	$2.53 \times 10^{-3}$	$2.53 \times 10^{-3}$
$\xi_{ext}$	$1.93 \times 10^{-4}$	$1.98 \times 10^{-5}$	$0.00 \times 10^{-1}$	$0.00 \times 10^{-1}$
	$SNR = 5dB$			
	$S = 1$	$S = 2$	$S = 3$	$S = 4$
$\xi_{tot}$	$4.15 \times 10^{-4}$	$2.20 \times 10^{-4}$	$1.30 \times 10^{-4}$	$1.30 \times 10^{-4}$
$\xi_{int}$	$3.31 \times 10^{-3}$	$2.76 \times 10^{-3}$	$2.09 \times 10^{-3}$	$2.09 \times 10^{-3}$
$\xi_{ext}$	$2.18 \times 10^{-4}$	$5.01 \times 10^{-5}$	$0.00 \times 10^{-1}$	$0.00 \times 10^{-1}$

Table I: *Inhomogeneous Square Object*,  $\ell = 1.5\lambda$ ,  $\tau = 0.02$  - Reconstruction errors: total ( $\xi_{tot}$ ), internal ( $\xi_{int}$ ) and external ( $\xi_{ext}$ ) errors.

	$SNR = 50dB$			
	$S = 1$	$S = 2$	$S = 3$	$S = 4$
$L^{(S)}$	6.00	1.50	1.50	1.50
$N^{(S)}$	100	148	148	148
$Q^{(S)}$	100	64	25	25
	$SNR = 20dB$			
	$S = 1$	$S = 2$	$S = 3$	$S = 4$
$L^{(S)}$	6.00	1.50	1.50	1.50
$N^{(S)}$	100	148	148	148
$Q^{(S)}$	100	64	25	25
	$SNR = 10dB$			
	$S = 1$	$S = 2$	$S = 3$	$S = 4$
$L^{(S)}$	6.00	1.50	1.50	1.50
$N^{(S)}$	100	148	148	148
$Q^{(S)}$	100	64	25	25
	$SNR = 5dB$			
	$S = 1$	$S = 2$	$S = 3$	$S = 4$
$L^{(S)}$	6.00	1.50	1.50	1.50
$N^{(S)}$	100	175	175	175
$Q^{(S)}$	100	100	25	25

Table II: *Inhomogeneous Square Object*,  $\ell = 1.5\lambda$ ,  $\tau = 0.02$  - Investigation domain parameters: restricted investigation domain size  $L^{(S)}$ , total number of cells  $N^{(S)}$  and number of cells within the restricted domain size  $Q^{(S)}$ .

### 1.1.2 Inhomogeneous Square Object, $\ell = 1.5\lambda$ , $\tau^{(1)} = 0.04$ - IMSA-BCS reconstructed profiles

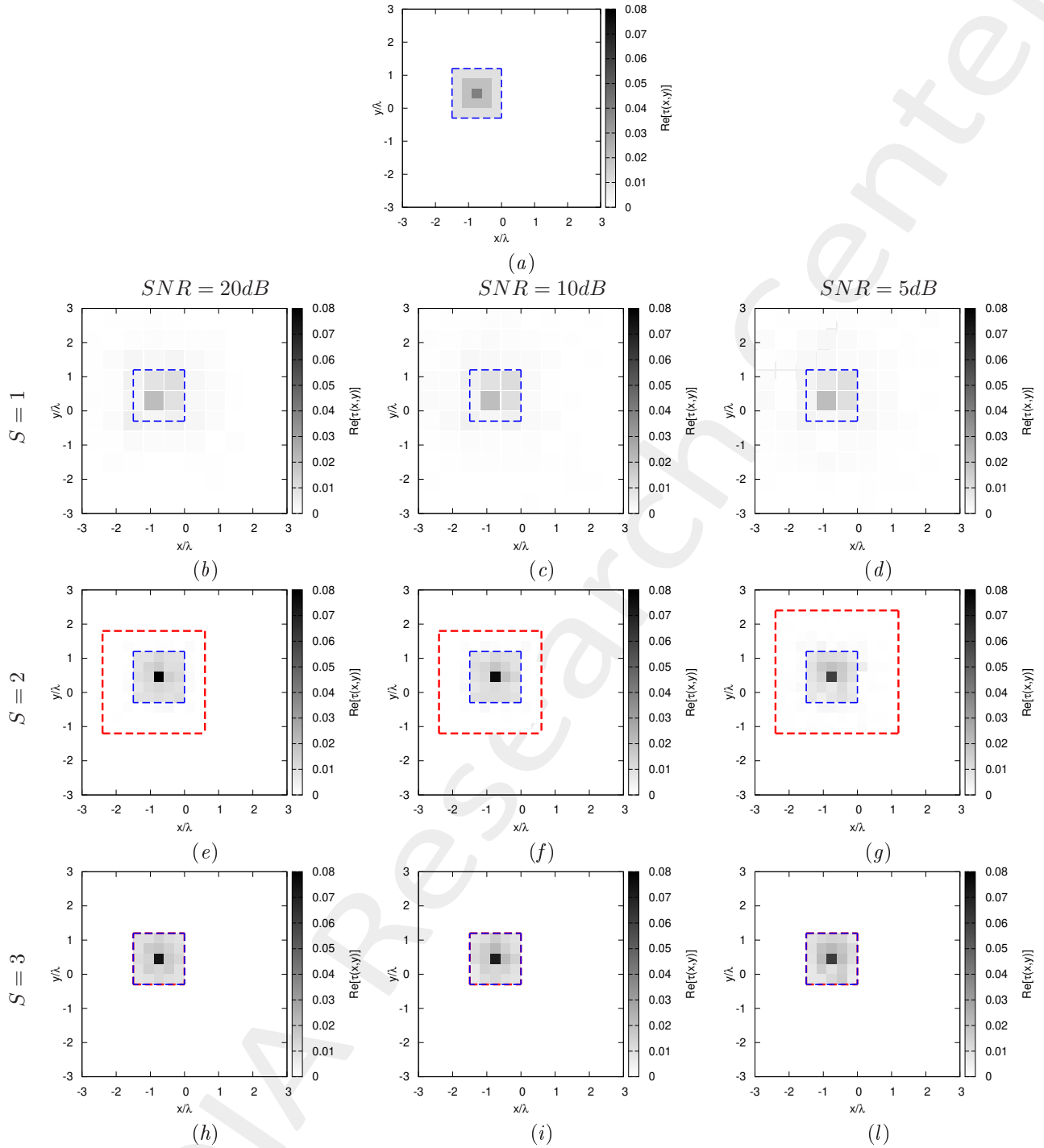


Figure 2: *Inhomogeneous Square Object*,  $\ell = 1.5\lambda$ ,  $\tau = 0.04$  - (a) Actual profile and (b)-(o) IMSA-BCS reconstructed profiles for (b)(e)(h)  $SNR = 20 \text{ [dB]}$ , (c)(f)(i)  $SNR = 10 \text{ [dB]}$  and (d)(g)(l)  $SNR = 5 \text{ [dB]}$  at the step (b)-(d)  $S = 1$ , (e)-(g)  $S = 2$ , and (h)-(l)  $S = 3$ .

	$SNR = 50dB$			
	$S = 1$	$S = 2$	$S = 3$	$S = 4$
$\xi_{tot}$	$9.35 \times 10^{-4}$	$3.25 \times 10^{-4}$	$2.14 \times 10^{-4}$	$2.14 \times 10^{-4}$
$\xi_{int}$	$5.22 \times 10^{-3}$	$4.44 \times 10^{-3}$	$3.42 \times 10^{-3}$	$3.42 \times 10^{-3}$
$\xi_{ext}$	$6.39 \times 10^{-4}$	$5.09 \times 10^{-5}$	$0.00 \times 10^{-1}$	$0.00 \times 10^{-1}$
	$SNR = 20dB$			
	$S = 1$	$S = 2$	$S = 3$	$S = 4$
$\xi_{tot}$	$9.36 \times 10^{-4}$	$3.26 \times 10^{-4}$	$2.13 \times 10^{-4}$	$2.13 \times 10^{-4}$
$\xi_{int}$	$5.15 \times 10^{-3}$	$4.43 \times 10^{-3}$	$3.41 \times 10^{-3}$	$3.41 \times 10^{-3}$
$\xi_{ext}$	$6.40 \times 10^{-4}$	$5.23 \times 10^{-5}$	$0.00 \times 10^{-1}$	$0.00 \times 10^{-1}$
	$SNR = 10dB$			
	$S = 1$	$S = 2$	$S = 3$	$S = 4$
$\xi_{tot}$	$9.57 \times 10^{-4}$	$3.19 \times 10^{-4}$	$4.84 \times 10^{-4}$	$2.33 \times 10^{-4}$
$\xi_{int}$	$5.09 \times 10^{-3}$	$4.14 \times 10^{-3}$	$7.75 \times 10^{-3}$	$3.72 \times 10^{-3}$
$\xi_{ext}$	$6.60 \times 10^{-4}$	$6.18 \times 10^{-5}$	$0.00 \times 10^{-1}$	$0.00 \times 10^{-1}$
	$SNR = 5dB$			
	$S = 1$	$S = 2$	$S = 3$	$S = 4$
$\xi_{tot}$	$1.08 \times 10^{-3}$	$4.22 \times 10^{-4}$	$2.13 \times 10^{-4}$	$2.13 \times 10^{-4}$
$\xi_{int}$	$5.50 \times 10^{-3}$	$3.93 \times 10^{-3}$	$3.36 \times 10^{-3}$	$3.36 \times 10^{-3}$
$\xi_{ext}$	$7.56 \times 10^{-4}$	$1.66 \times 10^{-4}$	$0.00 \times 10^{-1}$	$0.00 \times 10^{-1}$

Table III: *Inhomogeneous Square Object*,  $\ell = 1.5\lambda$ ,  $\tau = 0.04$  - Reconstruction errors: total ( $\xi_{tot}$ ), internal ( $\xi_{int}$ ) and external ( $\xi_{ext}$ ) errors.

	$SNR = 50dB$			
	$S = 1$	$S = 2$	$S = 3$	$S = 4$
$L^{(S)}$	6.00	1.50	1.50	1.50
$N^{(S)}$	100	175	175	175
$Q^{(S)}$	100	100	25	25
	$SNR = 20dB$			
	$S = 1$	$S = 2$	$S = 3$	$S = 4$
$L^{(S)}$	6.00	1.50	1.50	1.50
$N^{(S)}$	100	175	175	175
$Q^{(S)}$	100	100	25	25
	$SNR = 10dB$			
	$S = 1$	$S = 2$	$S = 3$	$S = 4$
$L^{(S)}$	6.00	1.50	1.50	1.50
$N^{(S)}$	100	175	175	175
$Q^{(S)}$	100	100	25	25
	$SNR = 5dB$			
	$S = 1$	$S = 2$	$S = 3$	$S = 4$
$L^{(S)}$	6.00	1.50	1.50	1.50
$N^{(S)}$	100	208	208	208
$Q^{(S)}$	100	144	25	25

Table IV: *Inhomogeneous Square Object*,  $\ell = 1.5\lambda$ ,  $\tau = 0.04$  - Investigation domain parameters: restricted investigation domain size  $L^{(S)}$ , total number of cells  $N^{(S)}$  and number of cells within the restricted domain size  $Q^{(S)}$ .

### 1.1.3 Inhomogeneous Square Object, $\ell = 1.5\lambda$ - Resume: Errors vs. $\tau^{(1)}$

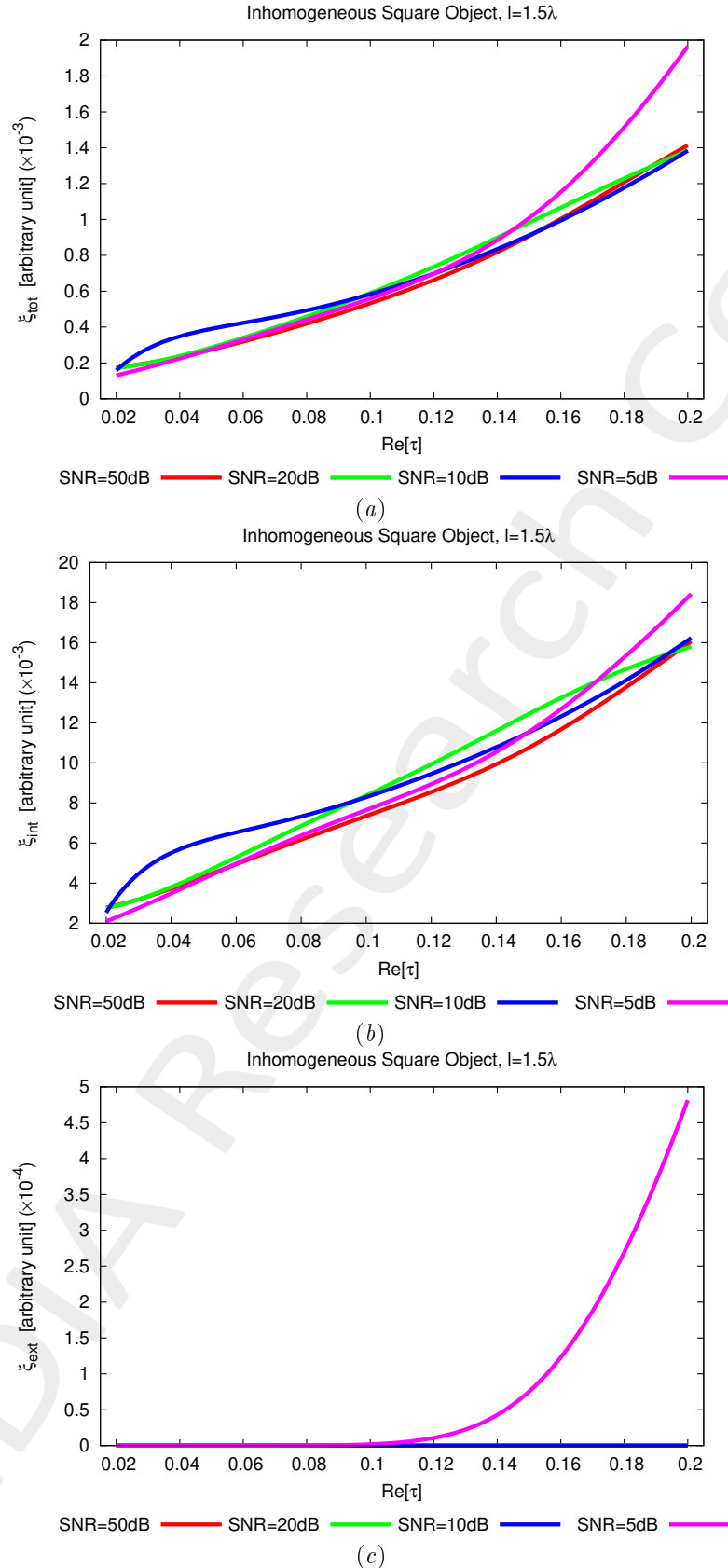


Figure 3: *Inhomogeneous Square Object,  $\ell = 1.5\lambda$  - Reconstruction errors vs.  $\tau$ : (a) total error, (b) internal error and (c) external error.*

#### 1.1.4 Inhomogeneous Square Object, $\ell = 1.5\lambda$ - Resume: Errors vs. SNR

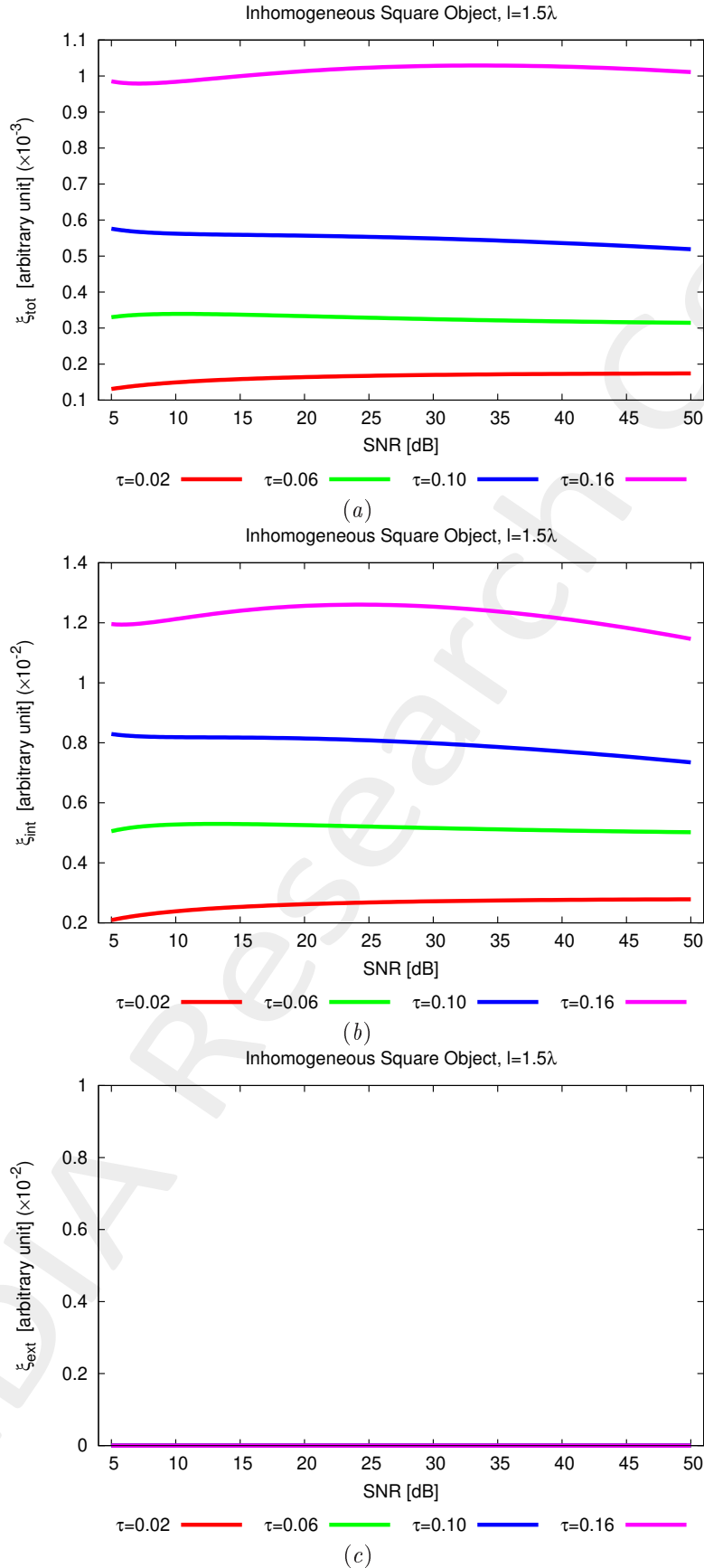


Figure 4: *Inhomogeneous Square Object,  $\ell = 1.5\lambda$*  - Reconstruction errors vs. SNR: (a) total error, (b) internal error and (c) external error.

### 1.1.5 Inhomogeneous Square Object, $\ell = 1.5\lambda$ - Resume: Errors vs. IMSA step, $S$

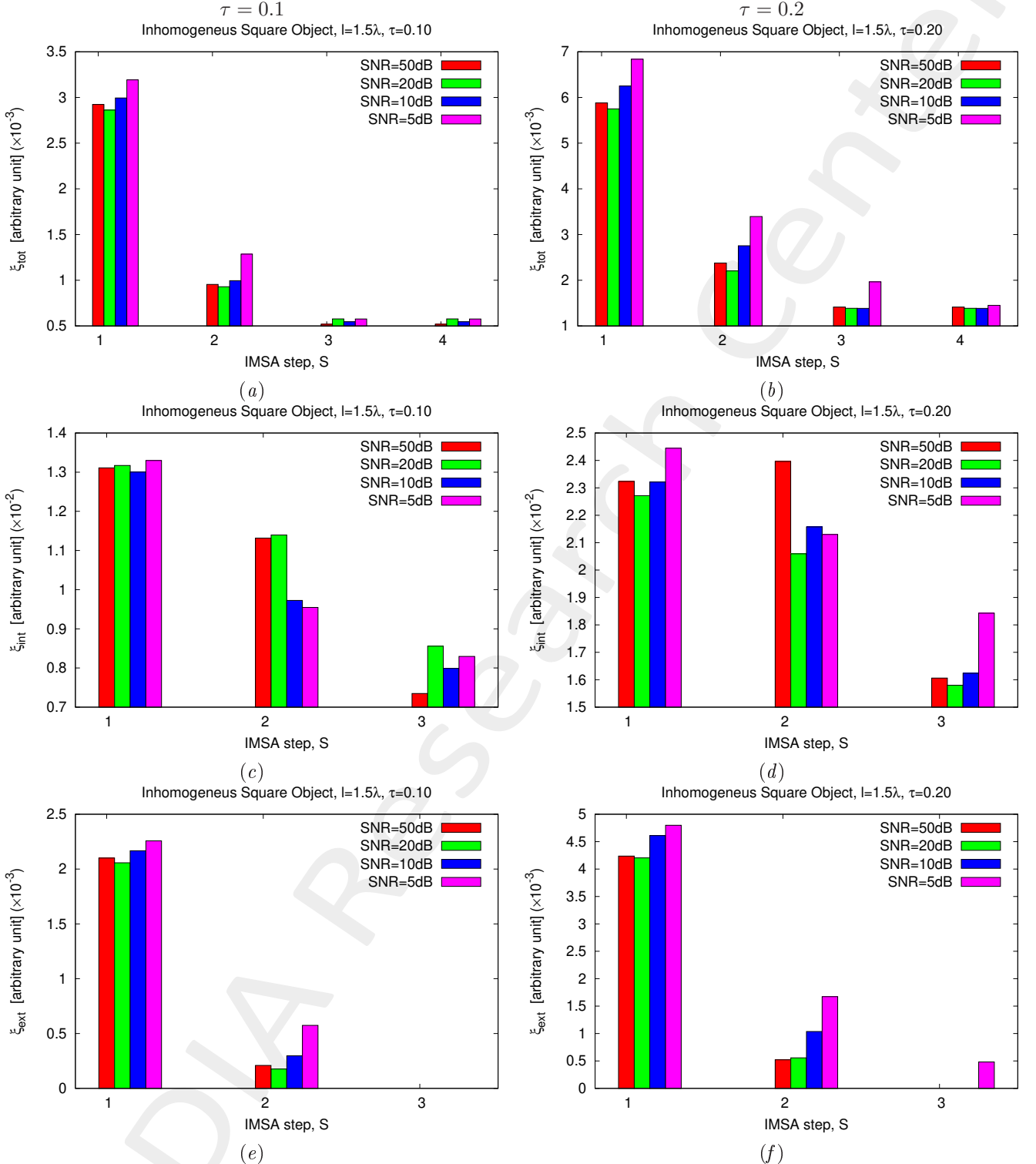


Figure 5: *Inhomogeneous Square Object,  $\ell = 1.5\lambda$  - Reconstruction errors vs. IMSA step,  $S$ :* (a)(b) total error, (c)(d) internal error and (e)(f) external error for (a)(c)(e)  $\tau = 0.1$  and (b)(d)(f)  $\tau = 0.2$ .

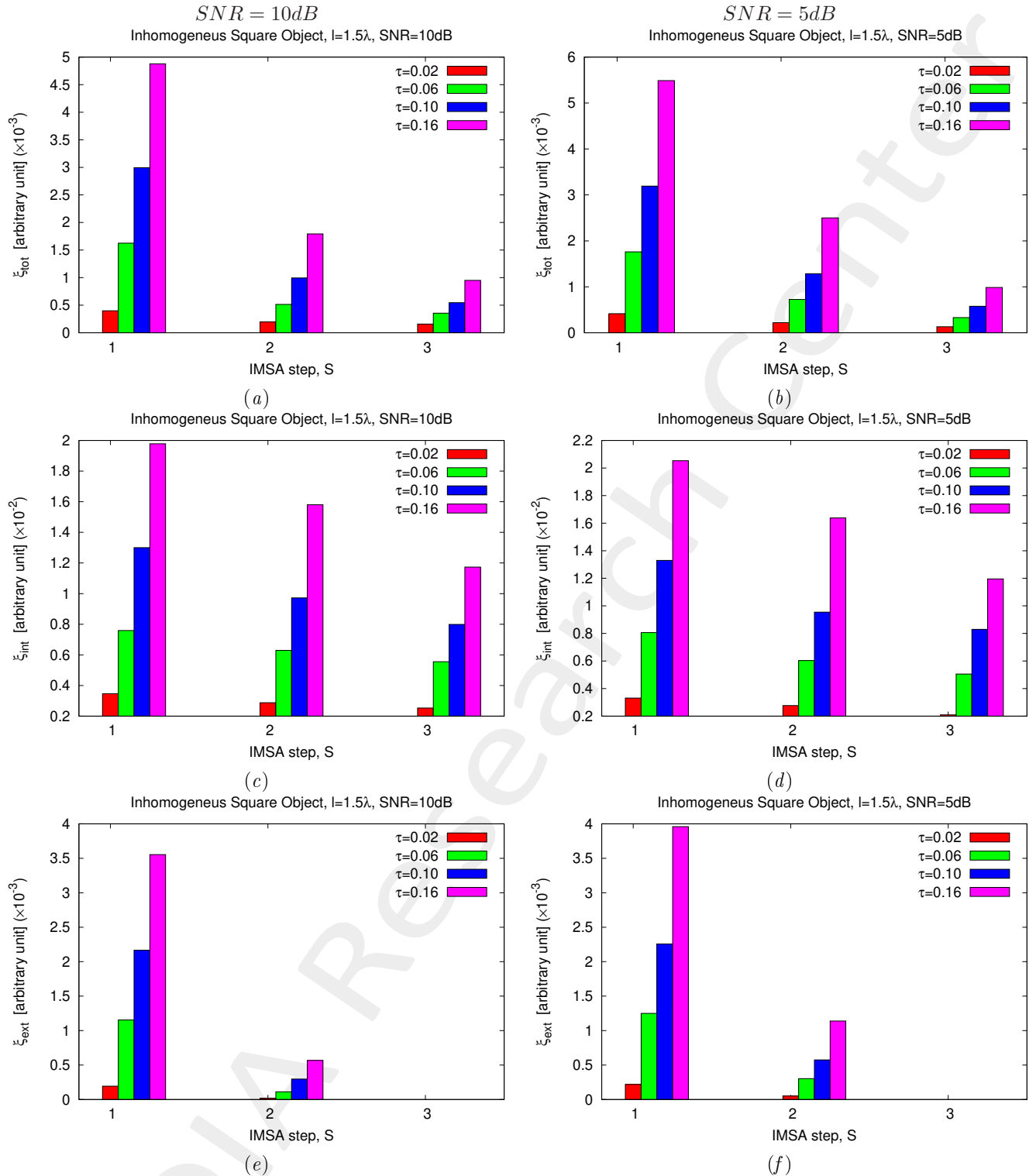


Figure 6: *Inhomogeneous Square Object*,  $\ell = 1.5\lambda$  - Reconstruction errors vs. *IMSA* step,  $S$ : (a)(b) total error, (c)(d) internal error and (e)(f) external error for (a)(c)(e)  $SNR = 10dB$  and (b)(d)(f)  $SNR = 5dB$ .

---

**More information on the topics of this document can be found in the following list of references.**

## References

- [1] M. Salucci, G. Oliveri, and A. Massa, "GPR prospecting through an inverse scattering frequency-hopping multi-focusing approach," *IEEE Trans. Geosci. Remote Sens.*, vol. 53, no. 12, pp. 6573-6592, Dec. 2015 (DOI: 10.1109/TGRS.2015.2444391).
- [2] M. Salucci, L. Poli, N. Anselmi, and A. Massa, "Multifrequency Particle Swarm Optimization for enhanced multi-resolution GPR microwave imaging," *IEEE Trans. Geosci. Remote Sens.*, vol. 55, no. 3, pp. 1305-1317, Mar. 2017 (DOI: 10.1109/TGRS.2016.2622061).
- [3] M. Salucci, L. Poli, and A. Massa, "Advanced multi-frequency GPR data processing for non-linear deterministic imaging," *Signal Processing - Special Issue on 'Advanced Ground-Penetrating Radar Signal-Processing Techniques,'* vol. 132, pp. 306-318, Mar. 2017 (DOI: 10.1016/j.sigpro.2016.06.019).
- [4] N. Anselmi, G. Oliveri, M. Salucci, and A. Massa, "Wavelet-based compressive imaging of sparse targets," *IEEE Trans. Antennas Propag.*, vol. 63, no. 11, pp. 4889-4900, Nov. 2015 (DOI: 10.1109/TAP.2015.2444423).
- [5] G. Oliveri, M. Salucci, N. Anselmi, and A. Massa, "Compressive sensing as applied to inverse problems for imaging: theory, applications, current trends, and open challenges," *IEEE Antennas Propag. Mag. - Special Issue on "Electromagnetic Inverse Problems for Sensing and Imaging,"* vol. 59, no. 5, pp. 34-46, Oct. 2017 (DOI: 10.1109/MAP.2017.2731204).
- [6] A. Massa, P. Rocca, and G. Oliveri, "Compressive sensing in electromagnetics - A review," *IEEE Antennas Propag. Mag.*, pp. 224-238, vol. 57, no. 1, Feb. 2015 (DOI: 10.1109/MAP.2015.2397092).
- [7] N. Anselmi, L. Poli, G. Oliveri, and A. Massa, "Iterative multi-resolution bayesian CS for microwave imaging," *IEEE Trans. Antennas Propag.*, vol. 66, no. 7, pp. 3665-3677, Jul. 2018 (DOI: 10.1109/TAP.2018.2826574).
- [8] N. Anselmi, G. Oliveri, M. A. Hannan, M. Salucci, and A. Massa, "Color compressive sensing imaging of arbitrary-shaped scatterers," *IEEE Trans. Microw. Theory Techn.*, vol. 65, no. 6, pp. 1986-1999, Jun. 2017 (DOI: 10.1109/TMTT.2016.2645570).
- [9] G. Oliveri, N. Anselmi, and A. Massa, "Compressive sensing imaging of non-sparse 2D scatterers by a total-variation approach within the Born approximation," *IEEE Trans. Antennas Propag.*, vol. 62, no. 10, pp. 5157-5170, Oct. 2014 (DOI: 10.1109/TAP.2014.2344673).
- [10] L. Poli, G. Oliveri, and A. Massa, "Imaging sparse metallic cylinders through a local shape function Bayesian compressive sensing approach," *J. Opt. Soc. Am. A*, vol. 30, no. 6, pp. 1261-1272, 2013 (DOI: 10.1364/JOSAA.30.001261).

- 
- [11] L. Poli, G. Oliveri, F. Viani, and A. Massa, "MT-BCS-based microwave imaging approach through minimum-norm current expansion," *IEEE Trans. Antennas Propag.*, vol. 61, no. 9, pp. 4722-4732, Sep. 2013 (DOI: 10.1109/TAP.2013.2265254).
  - [12] F. Viani, L. Poli, G. Oliveri, F. Robol, and A. Massa, "Sparse scatterers imaging through approximated multitask compressive sensing strategies," *Microwave Opt. Technol. Lett.*, vol. 55, no. 7, pp. 1553-1558, Jul. 2013 (10.1002/mop.27612).
  - [13] L. Poli, G. Oliveri, P. Rocca, and A. Massa, "Bayesian compressive sensing approaches for the reconstruction of two-dimensional sparse scatterers under TE illumination," *IEEE Trans. Geosci. Remote Sens.*, vol. 51, no. 5, pp. 2920-2936, May 2013 (DOI: 10.1109/TGRS.2012.2218613).
  - [14] L. Poli, G. Oliveri, and A. Massa, "Microwave imaging within the first-order Born approximation by means of the contrast-field Bayesian compressive sensing," *IEEE Trans. Antennas Propag.*, vol. 60, no. 6, pp. 2865-2879, Jun. 2012 (DOI: 10.1109/TAP.2012.2194676).
  - [15] G. Oliveri, L. Poli, P. Rocca, and A. Massa, "Bayesian compressive optical imaging within the Rytov approximation," *Optics Letters*, vol. 37, no. 10, pp. 1760-1762, 2012 (DOI: 10.1364/OL.37.001760).
  - [16] G. Oliveri, P. Rocca, and A. Massa, "A Bayesian compressive sampling-based inversion for imaging sparse scatterers," *IEEE Trans. Geosci. Remote Sens.*, vol. 49, no. 10, pp. 3993-4006, Oct. 2011 (DOI: 10.1109/TGRS.2011.2128329).
  - [17] G. Oliveri, M. Salucci, and N. Anselmi, "Tomographic imaging of sparse low-contrast targets in harsh environments through matrix completion," *IEEE Trans. Microw. Theory Tech.*, vol. 66, no. 6, pp. 2714-2730, Jun. 2018 (DOI: 10.1109/TMTT.2018.2825393).
  - [18] M. Salucci, A. Gelmini, L. Poli, G. Oliveri, and A. Massa, "Progressive compressive sensing for exploiting frequency-diversity in GPR imaging," *J.Electromagn. Waves Appl.*, vol. 32, no. 9, pp. 1164-1193, 2018 (DOI: 10.1080/09205071.2018.1425160).